

Supplemental Material for  
**Tropical convective transition statistics and causality in the water vapor-precipitation relation**

Yi-Hung Kuo, \* J. David Neelin, and C. Roberto Mechoso

*Department of Atmospheric and Oceanic Sciences, University of California Los Angeles, Los Angeles, CA, USA*

**Content of this file**

Lead-lag relationship between CWV and precipitation

Low-bias of NCEP Reanalysis CWV

References

Figures S1 to S3

**1. Lead-lag relationship between CWV and precipitation**

Figure 1 of the main text shows the composite time series centered at locally high *convective* precipitation using model output at Manus Island and the GOAmazon site for the standard entrainment case. Figure S1 shows the model composites similar to Fig. 1 of the main text, except that they refer to total precipitation. Here the composites are centered at locally high *total* precipitation (defined as being greater than the mean total precipitation rate averaged over all precipitating events with respect to the threshold value of  $0.1 \text{ mm hr}^{-1}$ ). There are some quantitative differences between composites in Figs. 1 and S1. For instance, the  $\widehat{q}_{sat}$  variation at the GOAmazon site has larger amplitude when composited on convective precipitation. This suggests that in the continental tropics, the diurnal cycle has more pronounced influence on convection than on the overall precipitation. At Manus Island, the total precipitation time series is rather symmetric in time-lag, and CWV very slightly leads the total precipitation maximum. After the total precipitation peaks, both  $\widehat{q}_{sat}$  and convective precipitation are smaller compared with before. Details aside, the behavior in Fig. S1 is highly consistent with the behavior seen in Fig. 1 based on convective precipitation.

**2. Low-bias of NCEP Reanalysis CWV**

It has been noted that the NCEP Reanalysis products consistently show a low bias for CWV over the tropical oceans (Trenberth and Guillemot 1998; Trenberth et al. 2005). Figure S2 shows the CWV climatology from RSS and Reanalysis-2 and their

difference. Figure S3 shows the CRH climatology calculated using the Reanalysis-2 temperature together with RSS and Reanalysis-2 CWV as well as the precipitation from the GPCP. From Figs. S2 and S3, regions with high (low) precipitation over the tropical oceans usually have high (low) CWV and CRH from satellite retrievals. Reanalysis-2 generally underestimates CWV in comparison with satellite microwave retrievals in regions where CWV is high, and slightly overestimates it in regions where CWV is low. This bias also results in the difference between Reanalysis-2 and RSS CRH. Overall, Reanalysis-2 underestimates CWV over the tropical oceans compared to satellite retrievals.

Given the evidence that the lack of entrainment in model physics leads to a drier atmosphere (see Figs. 2 and 3 of the main text), we can conjecture that the low CWV bias in the NCEP Reanalysis results from the entrainment process not being properly modeled in the Simplified Arakawa-Schubert scheme (or SAS scheme; Pan and Wu 1995) used in the atmospheric model component. In the SAS scheme, the level below 700 mb at which the moist static energy reaches local maximum is first found as the starting point (SP) of the convection in a model column. Then a parcel from the SP is taken upward, conserving its saturation moist static energy, to find the level of free convection (LFC, or cloud base). After the SP and LFC are found, the updraft mass flux is re-calculated by *assuming that entrainment occurs only between the SP and LFC, and 50% of the mass flux at the LFC originates at the SP*. The parcel is assumed to be non-entraining above LFC up to the cloud top. Thus the entrainment process is confined within a rather shallow layer instead of through the whole column. This suggests that a revision of the entrainment process might help to improve this aspect of the NCEP model and thus the reanalysis.

## References

- Trenberth, K. E., and C. J. Guillemot, 1998: Evaluation of the atmospheric moisture and hydrological cycle in the NCEP/NCAR reanalysis. *Climate Dyn.*, **14**, 213-231.
- Trenberth, K. E., J. Fasullo, and L. Smith, 2005: Trends and variability in column-integrated atmospheric water vapor. *Climate Dyn.*, **24**, 741-758.
- Pan, H.-L., and W.-S. Wu, 1995: Implementing a mass flux convective parameterization package for the NMC medium range forecast model. NMC Office Note 409, 40pp. [Available online at [www.emc.ncep.noaa.gov/officenotes/FullTOC.html#1990](http://www.emc.ncep.noaa.gov/officenotes/FullTOC.html#1990).]

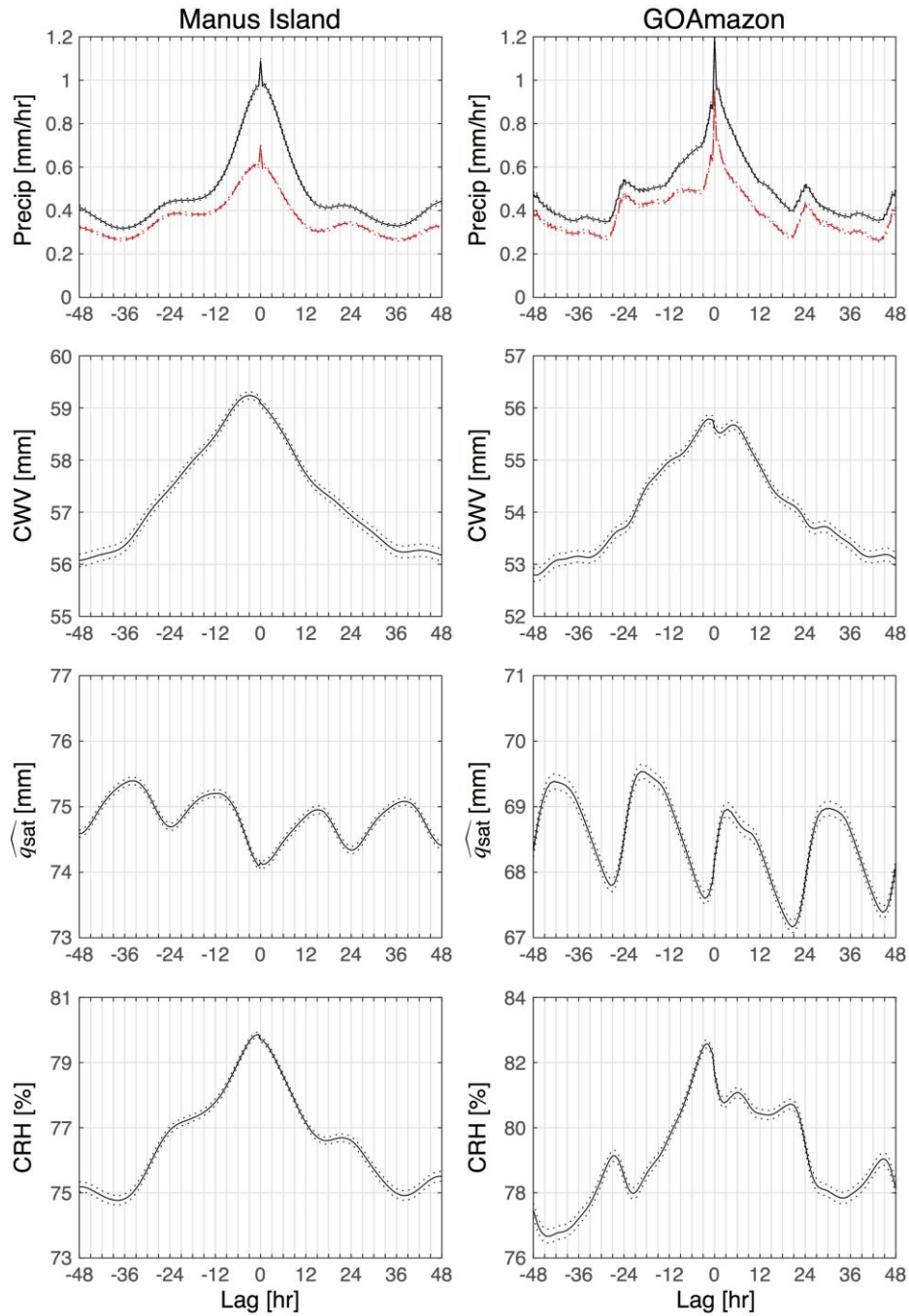


**Figure S1:** Model composite time series centered at locally high *total* precipitation (defined as being greater than the mean of all precipitating events with respect to the threshold of  $0.1 \text{ mm hr}^{-1}$ ) within a 96-hour window for standard entrainment case ( $\text{dmpdz}=1$ ). The top panels show the total (black) and convective (red) precipitation. Dotted curves in all panels represent  $\pm 1$  standard error. The qualitative features indicated by these curves are robust with respect to the threshold defining heavy precipitation.

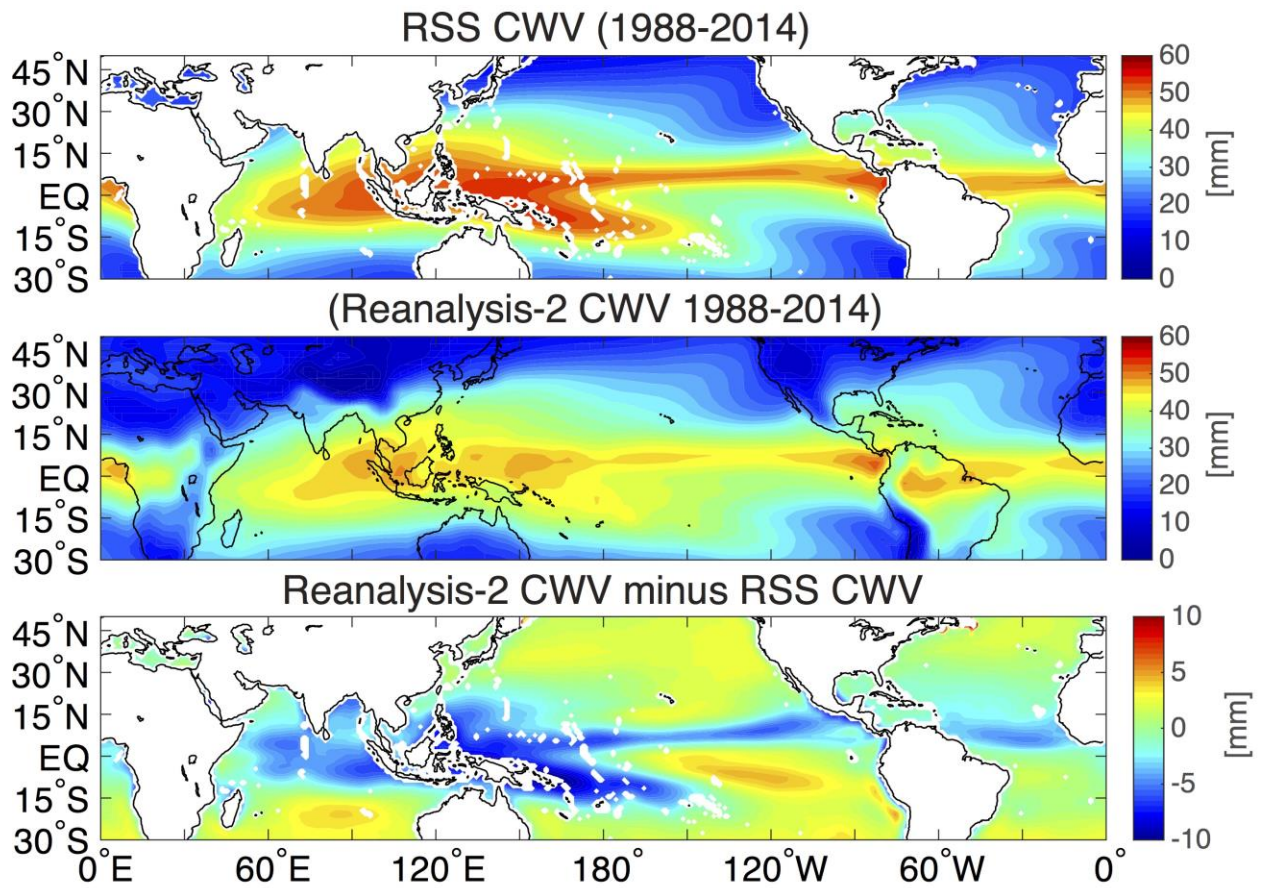


**Figure S2:** The climatology of CWV calculated using RSS CWV and Reanalysis-2 CWV (precipitable water). Their difference is plotted in the lower panel.

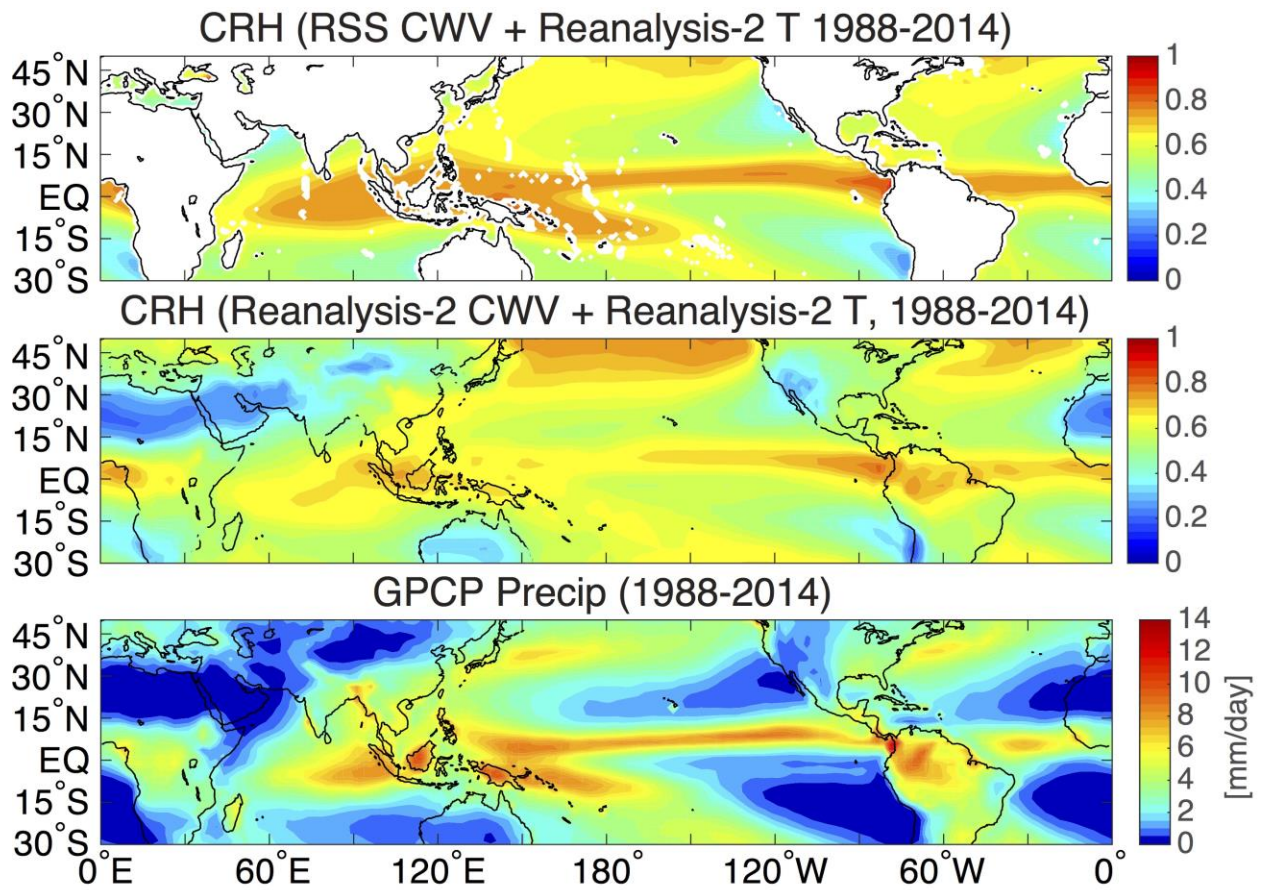


**Figure S3:** The climatology of CRH calculated using RSS and Reanalysis-2 datasets and precipitation from GPCP. The CRH values shown in the upper and middle panels are calculated using the RSS and Reanalysis-2 CWV, respectively. The Reanalysis-2 temperature field is used for both calculations.